Quasi-two-dimensional domain structures of magnetic particles in a static field

Y. H. Hwang and X-l. Wu
Department of Physics and Astronomy, University of Pittsburgh, Pittsburgh, Pennsylvania 15260
(Received 16 August 1993)

An array of magnetic-particle chains is assembled and aligned in a magnetic field H, and its structures are studied by small-angle light scattering. The system undergoes a series of structural changes: single particles $\rightarrow$ disordered anisotropical domains $\rightarrow$ array of strongly correlated columns, as H increases. Different structure regions are separated by two critical field lines $H_{C1}(\phi)$ and $H_{C2}(\phi)$, where ϕ is the concentration of the particles. Due to disorders inherited in the self-assembling process, the magnetic columns remain short-range ordered even in the strong-field limit, $H \gg H_{C2}$.

PACS number(s): 64.90.+b, 75.50.Mm, 82.70.Dd

Statistical mechanics of one-dimensional structures is interesting and has attracted much attention recently. Useful examples include Abrikosov flux lines in the type II superconductors [1], defect lines in liquid crystals [2], and grafted polymers [3]. In this paper we report another type of one-dimensional structure which arises when magnetic particles in an aqueous suspension are assembled and aligned in an external magnetic field. Using a small-angle light-scattering technique, we measured both the longitudinal and the transverse correlations of the magnetic chains. It has been found that the magnetic chains become increasingly more repulsive as the magnetic field H increases, giving rise to strong local ordering. However, in the strong-field limit, i.e., when the dipole-dipole interaction between the chains becomes much greater than the thermal energy k_BT, the system exhibits significant metastability and disorder on large scales. It appears that the long-range ordering, i.e., crystalline phase, of the chains is preempted by a glassy state.

A close cousin of the system under investigation is that of an electrorheological fluid, which has been studied extensively due to its intriguing physical properties and a great potential for commercial applications [4–6]. When an electrostatic field is applied to the electrorheological fluid, the dielectric particles, typically glass beads immersed in oil, also aggregate, producing tenuous strings in early times. Being essentially a one-dimensional object imbedded in three-dimensional space, an aligned particle chain experiences strong conformational fluctuations, known as Landau-Peierls instability [7]. It has been suggested [8] recently that the conformational fluctuations can induce an attractive force which causes the chains to migrate, producing thick columnar structures at later times. According to this theory the electrorheological fluid in a strong field is unstable with respect to long-wavelength density fluctuations ($q \rightarrow 0$), and the equilibrium state of the system corresponds to a complete phase separation with particles clumping to a giant cluster. From an energetic consideration ($T = 0$), it was further suggested that the ground state has a FCC lattice structure [9]. Certain features of the theories have been born out by recent experiments using small-angle light scattering, by Martin, Odinek and Halsey [5], and laser diffraction, by Chen, Zitter and Tao [10].

Our observations of magnetic particles in a static magnetic field differ somewhat from these theoretical pictures. The differences may stem from the following two effects which we believe to have been somewhat overlooked in the past. First, we noted that the key assumption in the calculation of electrorheological fluid is that the length of the particle chains is infinite [8, 9]. This is consistent with the experimental situations in which the particles are confined between two parallel electrodes, which behave as perfect conductors. Multiple reflections of image charges in the electrodes make a finite chain behaving essentially as an infinite chain. For this reason, the electric dipole moments along the chain are mutually screened by their neighbors. Namely, for a test magnetic dipole situated next to the chain, the interaction between the dipole moment and the chain decays exponentially with a decay length being of the order of the particle diameter. For a collection of these dipolar chains, therefore, the interactions between them are also short ranged, with the long-range part, which is due to the monopole-monopole interactions, being isolated at infinity and negligible. In our system, since the glass walls are nonmagnetic, there are no image "charges" for the magnetic dipoles. Hence the length of the chains remains finite, and the interactions between the chains are dominated by the long-ranged repulsive dipole interactions, which prevent the chains from aggregating. Second, due to the stochastic nature of chain formation, the interactions between the chains are random. As a result the system shows a great deal of disorder and hysteretic effects. The large scale motions of chains are frozen out as the magnetic field increases. Therefore the kinetics of the system also inhibits coarsening of the chains [11].

Aqueous magnetic particles were purchased from Seradyn, Inc. [12]. These are polystyrene spheres which have an average diameter of $D \approx 0.9$ μm and contain multigrain ferromagnetic cores. Since the magnetization of individual grains is randomly oriented, the polystyrene sphere possesses no net magnetization in zero field. The particles are stabilized by surface charge groups (carboxylic acid), and show reversible aggregation behavior. The stock solution contains $\phi = 10\%$ solid volume frac-

tion, and other concentrations for the experiment were prepared by diluting the stock solution using distilled water. In order to maintain uniform particle concentration, all the samples were sonicated for several minutes before the measurements.

The magnetic-particle solution was contained between two optical flats ($\lambda/10$) and sealed under compression in a stainless steel holder. The optical flats were separated by nylon gaskets whose thicknesses were varied between $L = 10$ and 30 μm. Because of the large sized particles used, thin samples are necessary in order to reduce multiple-scattering contribution to the light-intensity measurements. The prepared sample was placed in the center of a Helmholtz coil pair with a dc magnetic field H, which can be varied up to about 100 G.

Small-angle light-scattering measurements were carried out to probe the magnetic domain structures. As shown in Fig. 1, a 5 mW He-Ne laser beam ($\lambda = 632.8$ nm) is expanded to a diameter of ~ 2 cm by a spatial filter assembly. In normal operations, the input laser impinges normally on the sample and the scattered light is projected onto a translucent screen by a convex lens L_2. The use of an expanded laser beam and L_2 greatly reduce the speckle size of the scattered light, making the intensity measurement more reliable. In this scattering geometry, the apparent scattering angle θ_m is related to the focal length f of L_2 by $\theta_m = \arctan(r/f)$, where r is the radial position on the screen. However, due to the mismatch in the refractive indexes of water and air, the actual scattering angle θ_s is different from θ_m and is given by

$$\theta_s = \sin^{-1}\left(\frac{\sin\theta_m}{n}\right),$$

where $n = 1.33$ is the refractive index of water. For a given input wave vector $k_0 = \frac{2\pi n}{\lambda}$, the scattering wave vector is related to k_0 by $q = 2k_0 \sin(\theta_s/2)$. For $f = 20$ cm, a range of scattering angles, $2° < \theta_s < 10°$, is accessible, corresponding to a range of scattering wave vectors, $4000 < q < 20\,000$ cm^{-1}. Since $q \ll k_0$, $\vec{q}$ is almost perpendicular to the optical axis. As indicated in Fig. 1, the sample cell together with the Helmholtz coils can be rotated along the x axis by an angle Ψ. For $\Psi = 0$, the input laser impinges normally on the sample; $\vec{q}$ is in the x-y plane. Therefore the setup measures the in-plane concentration fluctuations of the particles. For $\Psi \sim 90°$, $\vec{q}$ is nearly normal to the sample so that it probes anisotropic scattering in the x-z plane. The scattering intensity distribution on the screen is measured by a charge-coupled device (CCD) camera and digitized at a resolution of 540 (horizontal) $\times$ 480 (vertical) pixels. Various corrections due to finite projection angles on the CCD and optical aberrations were considered. It was found that while these corrections are significant for absolute scattering intensity measurements, they are insignificant for determining the location of $q_{\max}$, which is the primary interest of this paper.

For small magnetic fields, particles interact weakly and their positions are random due to thermal fluctuations. In this weak-field limit, the scattering intensity distribution is isotropic in all directions, indicating no chain formation. As H increases and passes a certain threshold, H_{C1}, an onset of optical anisotropy is observed in the x-z plane. The anisotropic scattering is readily observable by rotating the sample assembly (sample plus Helmholtz coil) by an angle $\Psi \sim 90°$, with H pointing along the z axis. The anisotropic scattering starts as an ellipsoid and evolves into a bright line as H increases. Figure 2 shows the scattering intensity distribution, $I(q_x, q_z)$, with a field slightly greater than H_{C1}. We noted that as H increases the greatest change in scattering intensity distribution, $I(q_x, q_z)$, is along the x direction, while the scattering intensity along the z direction is nearly unaffected. The scattering pattern indicates that above H_{C1} the particles are aggregated and formed elongated domains with their long axis parallel to H.

By measuring the onset of the optical anisotropy as a function of ϕ, we found that $H_{C1}(\phi)$ decreases monotonically with ϕ. Two sets of measurements were carried out with different sample thicknesses $L/D = 13$ (circles) and 34 (squares), as shown in Fig. 3. The experimental data can be fit approximately to a power law $H_{C1} \sim \phi^{-\alpha_1}$ with $\alpha_1 \simeq 1/4$ for both measurements. Besides the concentration dependence, a remarkable increase in $H_{C1}(\phi)$ was also observed as the sample thickness L/D decreases. The behavior is interesting in that it clearly demonstrates the long-range nature of dipole-dipole interaction, and its strong influence on the onset of chain formation [13].

Despite ordering, or chaining, along the field direction, in the neighborhood of $H_{C1}(\phi)$ the in-plane scattering intensity distribution, $I(q_x, q_y)$, is isotropic and peaks in the forward direction ($q \to 0$). This indicates that the elongated magnetic domains are uncorrelated in the x-y plane and the structure of the magnetic fluid resembles that of a quasi-two-dimensional gas. However, by gradually increasing H, the forward scattering intensity decreases and a second scattering peak emerges at a finite q ($= q_{\max}$) value. Figure 4 shows a sequence of $I(q_x, q_y)$

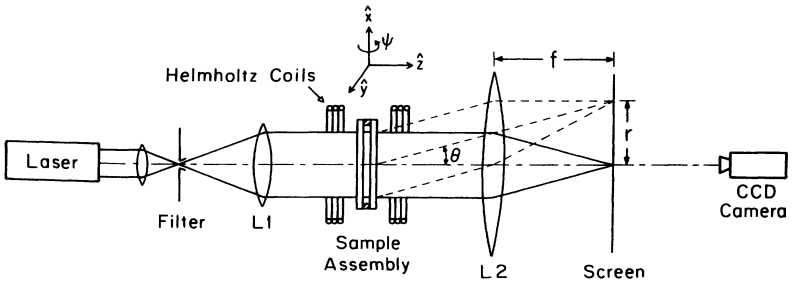

FIG. 1. Small-angle light scattering apparatus.

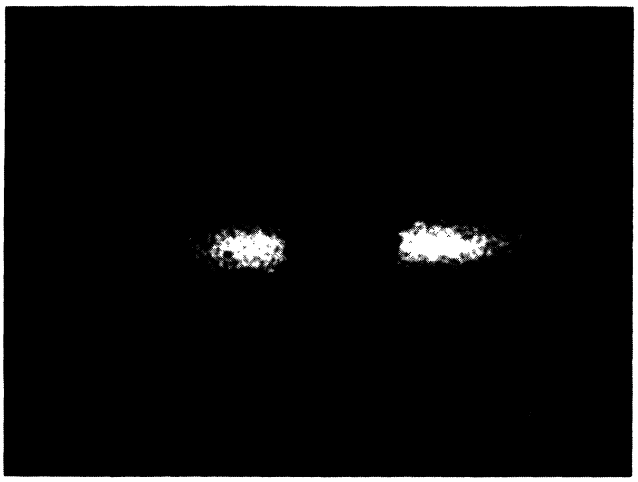

FIG. 2. Anisotropic scattering in the x-z plane. The concentration of the sample is $\phi = 5\%$ and the dimensionless sample thickness is $L/D = 25$. The optical anisotropy is a result of particle chaining along the z direction (vertical direction). The field (4 G) is applied adiabatically.

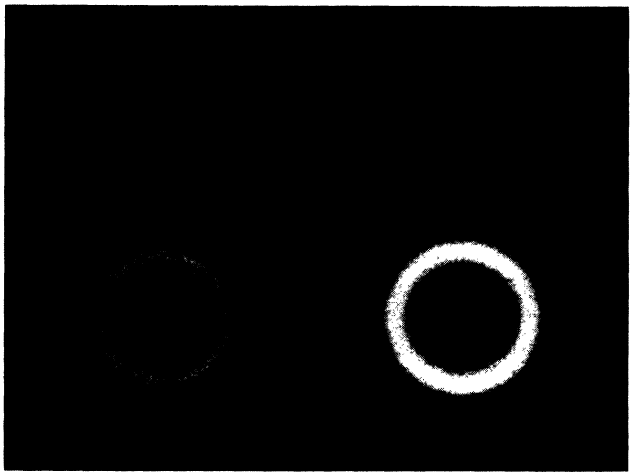

FIG. 4. The scattering intensity distribution in the x-y plane. The concentration of the sample is $\phi = 5\%$ and the sample thickness is $L/D = 25$. The magnetic field is applied adiabatically.

at $H = 0$, 10, 20, and 40 G for a sample with $\phi = 5\%$ and $L/D = 25$. Since the forward scattering intensity is proportional to the osmotic compressibility of the fluid, the decreasing scattering intensity at small q indicates that the interaction between the domains is repulsive and its strength increases with H, i.e., the magnetic fluid becomes less "compressible" in a stronger field. The repulsive interaction must also be responsible for the observed in-plane correlation between the domains, which gives rise to the distinctive second scattering peak at $q_{\max}$.

The appearance of the scattering peak at finite q values allows us to define, phenomenologically, a second critical field line $H_{C2}(\phi)$. Physically this quantity measures the relative strength of in-plane domain-domain interaction to that of thermal energy k_BT. We found that H_{C2} also decays monotonically as a function of ϕ, $H_{C2} \sim \phi^{-\alpha_2}$, but with the exponent $\alpha_2 \simeq 1/2$, which is a factor of 2 greater than α_1, as shown in Fig. 3. Unlike $H_{C1}(\phi)$, which depends strongly on the thickness of the sample, $H_{C2}(\phi)$ appears to have weak or no sample-thickness dependence [14]. Furthermore, we noted that the two critical field lines, H_{C1} and H_{C2}, appear to merge at sufficiently high concentrations.

An interesting feature of our small-angle light-scattering measurements is that above H_{C2}, $q_{\max}$ increases with H and saturates at certain values q_0. This behavior has been observed for all the samples with different concentrations ϕ and sample thickness L/D. Figure 5 shows a plot of $q_{\max}$ vs ϕ and H for samples with $L/D = 13$. If a saturation field H_S is assigned to the crossover regime where $q_{\max}$ begins to level off for each

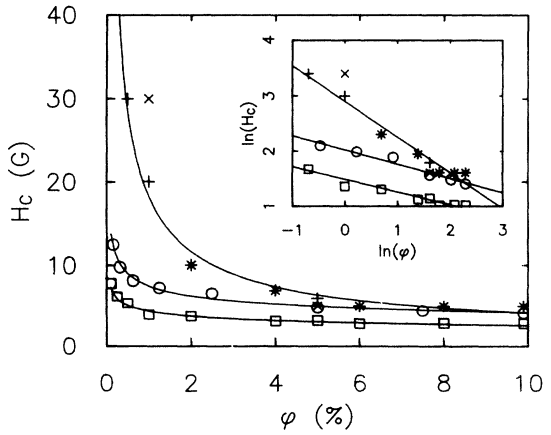

FIG. 3. H_{C1} and H_{C2} vs ϕ. The circles and squares are the measurements for the first critical field lines H_{C1} with $L/D = 13$ and 34, respectively. The pluses and crosses are the measurements for the second critical field lines H_{C2} with $L/D = 13$ and 34, respectively. The inset is a log-log plot of the same figure.

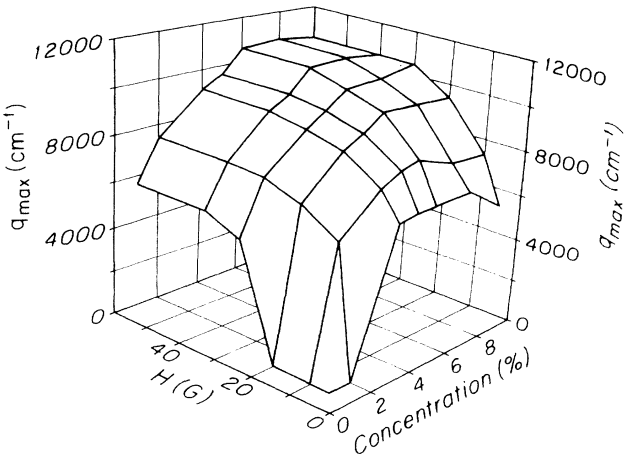

FIG. 5. The $q_{\max}$ vs H and ϕ. The $q_{\max}$ increases as either H or ϕ increases and saturates at $\sim 1 \times 10^3$ cm^{-1}. For a weak H and low concentrations, $q_{\max} \simeq 0$.

ϕ, we found that H_S is nearly independent of ϕ. In the strong-field limit, $H > H_S$ ($> H_{C2}$), the scattering intensity distribution becomes independent of H, and the structure of the magnetic fluid appears to be completely frozen.

What are the causes for q_{max} to increase as H increases? Naively one would expect that q_{max} is inversely proportional to the average distance L_s between the magnetic domains. Therefore an increase in q_{max} must be accompanied by a decrease in L_s, indicating that the domains become more crowded as H increases. However, this turned out not to be the case. Visual observations using a $\times 500$ microscope showed that even though the magnetic domains (columnlike structures) form at a relatively early stage with $H \sim H_{C1}$, above H_{C2} the number density of the domain, hence L_s, is essentially fixed. It appears that the net effect of increasing H in this region is that the individual domains becomes more compact, with decreasing radius, and the lateral correlation between the domains becomes stronger. Since the light-scattering intensity at a given q is the multiplication of the form factor $P(q)$ and the structure factor $S(q)$ of the fluid, i.e., $I(q) \sim P(q)S(q)$, it is not surprising that q_{max} moves to a higher value as the domain size δR decreases. A simple scaling argument [15], assuming that there are only two relevant length scales in the problem, namely, L_s and δR, gives $q_{max}/q_0 = F(\delta R^2/L_s^2)$, where $F(x)$ is an arbitrary scaling function. In accordance with the conjecture of Landau-Peierls instability [7,8] we may set δR to be proportional to the amplitude of lateral fluctuations of the magnetic chains $\delta\rho$, with $\langle \delta\rho^2 \rangle \sim (L/D)k_BTD^3/\mu^2 q^2$, where $\langle\ \rangle$ indicates an ensemble average and μ is the induced magnetic dipole moment, which is proportional to H. This gives $\delta R^2/L_s^2 \sim \phi/H^2$. The above scaling argument appears to work reasonably well for our light-scattering measurements as shown in Fig. 6. Here the data are taken directly from Fig. 5, which consists of six different concentrations, and the solid line in the figure is a guide to the eye.

A quantity of both practical and theoretical interests is the average number of chains N_{ch} per column at equilibrium. This quantity can be most easily calculated in the strong-field limit, $H \gg H_{C2}$, since in this regime the domains are locally packed in a hexagonal fashion, and all the particles are assembled into the domains. Using the fact that $q_0 \sim 1/L_s$, L_s is inversely proportional to the square root of the chain density, and the total number of particles is conserved, we found $N_{ch} = 6\sqrt{3}\pi\phi/D^2q_0^2$. Applying the measured value q_0 for each concentration ϕ, we found that N_{ch} depends linearly on ϕ, with $N_{ch} \sim 1$ at low concentrations and ~ 3 at high concentrations, as shown in the inset of Fig. 6. The measurements by the light-scattering technique are consistent with the visual observations using the optical microscope [16]. We note, however, that these observations are quantitatively different from those seen in electrorheological fluids in that the domains in our system are small and compact. And most importantly, they do not coalesce over time. In comparison, the domains in the electrorheological fluids are connected with random interfaces, resembling that of spinodal decomposition patterns. As a result, the two-dimensional Porod law was observed in a recent scattering experiment, in which the scattering intensity was found to decay as $1/q^3$ at large scattering wave vectors [5, 17]. The random interfaces seen in the electrorheological fluid were interpreted as a signature of fluctuation-induced coupling which causes the chains to collapse, forming large, continuous domains.

The above observations allow us to construct a quantitative structure phase diagram for the magnetic fluid. As shown in Fig. 7, for a fixed concentration ϕ, the system undergoes a series of structure changes: single particles (SP) $\rightarrow$ elongated disordered domains (EDD) $\rightarrow$ array of correlated columns (CC), as H increases. The different structure regimes are separated by two critical field lines, H_{C1} and H_{C2}, corresponding to the onset of longitudi-

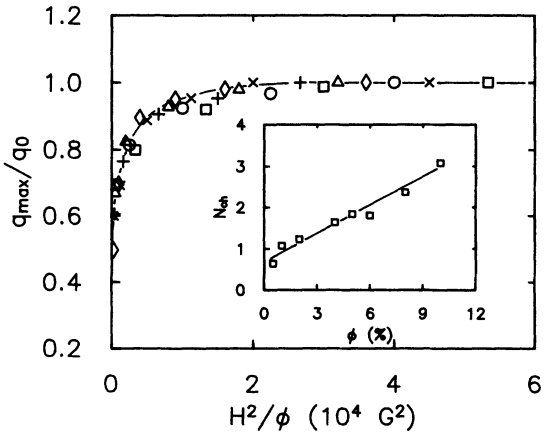

FIG. 6. The scaling behavior for q_{max}/q_0. The measurements are made in the strong-field limit, $H \gg H_{C2}$. The inset shows the number of chains per column vs the particle concentration ϕ.

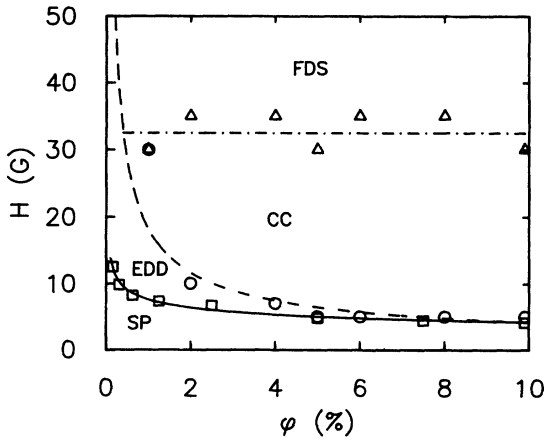

FIG. 7. The structure phase diagram of magnetic fluid. The symbols SP, EDD, CC, and FDS stand for single particle, elongated disordered domains, correlated columns, and frozen-domain states, respectively. The solid line indicates the first critical field line $H_{C1}(\phi)$, the dashed line indicates the second critical field line $H_{C2}(\phi)$, and the dash-dotted line indicates the saturation field line H_S. The measurement is for the sample with $L/D = 13$.

nal and transverse correlations. In the strong-field limit, $H \gg H_{C2}$, the system contains tenuous columns whose thickness is of the order of a few particle diameters. In this regime no macroscopic structure rearrangement was observed over several hours and the system appears to be locked in a frozen-domain state (FDS), or glassy state.

The measurements reported above were all performed at equilibrium conditions. Namely, H is varied adiabatically, allowing the system to relax after each small increment of H. Nonequilibrium measurements were also carried out in which H was changed abruptly from an initial value H_i to a final value H_f [18]. For a sufficiently deep quench, the scattering intensity distribution $I(q_x, q_y)$ also exhibits a structure peak $q_{\max}$. However, the position, the width, and the intensity of the peak depend critically on the history and the quenching depth of the applied field. For instance, raising H rapidly from 0 to 60 G gives rise to a weaker, broader peak, and $q_{\max}$ moves to a higher value as compared to the equilibrium measurement with the same final field strength. Likewise, quenching to 60 G in two separate steps produces yet another different structure. Figure 8 shows a series of measurements of $q_{\max}$ with various quenching depth, ranging from H_f =5 to 60 G for $H_i = 0$. As can be seen, the difference between the equilibrium and the nonequilibrium measurements becomes more distinctive as the quenching depth increases. The kinetics of the domain formation is also interesting. It has been found that the domains grow rapidly, and within a couple of seconds after the quench the formation is essentially completed. Despite a remarkable increase in the peak intensity, the position of $q_{\max}$ nevertheless remains constant during the formation period, as shown in Fig. 9. This behavior is again quantitatively different from the electrorheological fluids [5, 17] in that the scattering intensity distribution in the electrorheological fluids evolves slowly, on the order of a few hundred seconds, and $q_{\max}$ moves towards smaller values. The slow kinetics seen in the electrorheological fluids was interpreted as coarsening of domains due to the weakly fluctuating force, similar to that of van

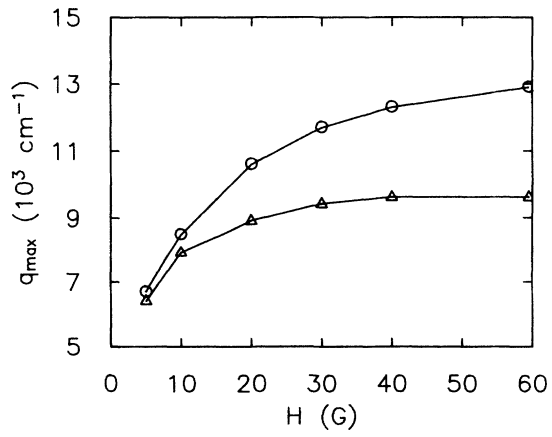

FIG. 8. The equilibrium and nonequilibrium $q_{\max}$ measurements. The measurements are performed with $\phi = 5\%$ and $L/D = 13$. The triangles and the circles are for the equilibrium and the nonequilibrium measurements, respectively.

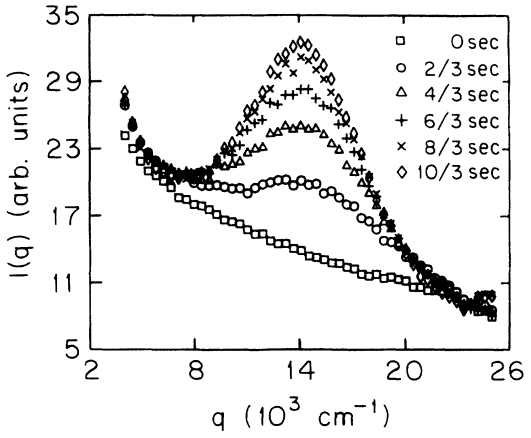

FIG. 9. Evolution of magnetic domain structures. The measurement was performed in a sample with $\phi = 5\%$ and $L/D = 13$. The sample was quenched from 0 to 50 G. The radial distribution of scattering intensity $I(q)$ was obtained by a circular integration, or averaging, over a constant wave vector q in the x-y plane. Note that despite large increases in the scattering intensity, the position of the scattering peak $q_{\max}$ remains constant in time.

der Waals interaction [5, 17]. Experimentally the domain growth was found to obey a power-law behavior with $R \sim t^{0.42}$, in qualitative agreement with the theory [17]. The lack of the coarsening behavior in our magnetic fluid therefore provides yet another indication that the interaction between the domains is predominantly repulsive.

The above measurements suggest that the magnetic domains are significantly more disordered by rapid quenching than by slowly increasing the field. Furthermore, since in the equilibrium measurements the columns are already thin, consisting approximately of a single chain, the nonequilibrium measurements, with smaller values of $q_{\max}$ and broader peaks, imply that a significant fraction of the particles form incomplete chains whose length varies between D and L. The enhanced disorder in the x-y plane may be a direct consequence of the broad distribution of chain length. The nonequilibrium structure that we observed seems to have very long lifetimes. Under the optical microscope, we found that large scale motions of the magnetic chains are completely frozen for $H_f \gg H_{C2}$. We were not able to detect structure relaxation and coarsening of chains over a period of 12 h. The long lasting metastability suggests that the energy barrier for the structure relaxation is much greater than the thermal energy, k_BT, and the system is essentially trapped in a local minimum of a free energy.

One of the interesting findings of our experiment is that the frozen-domain state preempts the long-range ordering (crystalline phase) of the system. The behavior is significantly different from a single layer of magnetic particles in a field perpendicular to the layer. In this case a crystalline phase with long-range hexagonal packing was observed [19]. Our experiment therefore suggests that the extra degrees of freedom, by allowing the particles to assemble along the field direction, and the fluctuations resulting from such degrees of freedom are responsible for

the disordered structures that we observed [11]. Specifically, these fluctuations may include thermally excited waves along the chains and "dislocations" in the chains as a result of self-assembly process. It remains an intriguing possibility that the fluctuations may be harnessed to produce various degrees of disorder in the magnetic domains, by varying the quenching rate, the sample size, and the concentration of the particles.

The concentration dependence of H_{C1} that we measured is quantitatively different from a previous measurement for a similar system [20]. Using an optical transmission measurement Lemaire *et al.* found that the turbidity increases sharply upon reaching a certain field strength and they interpreted the sharp increase as the onset of the aggregation. Their measurement indicated that H_{C1} is a linear increasing function of ϕ instead of a decreasing function of ϕ, as reported in this paper. Since the turbidity is an integral of partial scattering cross section, it may not be sensitive to a particular structure in the magnetic fluid. On the other hand, in our experiment the anisotropic scattering directly probes the uniaxial growth of the particle chains, and the technique is likely to be the most accurate means of determining H_{C1}. Qualitatively, our observation of H_{C1} is consistent with the second virial coefficient calculation [11] which predicts

$$H_{C1}^2 = \frac{12k_BT}{\pi^2\chi^2\phi(1-\phi)^2D^3[7+2(L/D)+12(L/D)^2]} ,$$

where χ is the magnetic susceptibility of the particle. This expression shows that H_{C1} is a decreasing function of both ϕ and L/D, as seen in our experiment. Quantitatively, however, the calculated H_{C1} does not agree with the experimental observations. Notably, the exponent α_1 is a factor of 2 greater than that observed in the experiment. The cause of the discrepancy is not clear at present.

To summarize, we performed small-angle light-scattering measurements to probe domain structures of an aqueous magnetic-particle suspension in a parallel-plate geometry. We found that the magnetic particles undergo a series of structure changes: single particles $\rightarrow$ elongated disordered domains $\rightarrow$ transversely correlated columns, as H increases. The various structure regions are separated by two critical field lines H_{C1} and H_{C2}. It appears that above H_{C2} the system spontaneously orders into a state which can be characterized by two length scales, the size of the columns δR and the average separation L_s between the columns. Several of our measurements, both static and dynamic, suggest that the interaction between the columns is predominantly repulsive, which is qualitatively different from electrorheological fluids. In the strong-field limit $H \gg H_{C2}$ the magnetic columns contain approximately a single chain and their lateral positions are frozen. In this frozen state, the array of magnetic chains is locally ordered but globally disordered. Associated with the disorder, the system exhibits interesting metastability and hysteretic effects. Many features observed in the experiment indicate the system falls out of thermal equilibrium quickly as H increases and behaves essentially as a two-dimensional glass.

We are grateful to W. I. Goldburg, M. Widom, and C. Yeung for their useful comments and suggestions on the experiment. This work was partially supported by the American Chemical Society under Grant No. PRF 26567-AC9, and a grant from Exxon Co.

[1] M.P.A. Fisher, Phys. Rev. Lett. **62**, 1415 (1989); D.S. Fisher, M.P.A. Fisher, and D.A. Huse, Phys. Rev. B **43**, 130 (1991).

[2] I. Chuang, N. Turok, and B. Yurke, Phys. Rev. Lett. **66**, 2472 (1991).

[3] S.T. Milner, Science **51**, 251 (1991); S.T. Milner, T.A. Witten, and M.E. Cates, Europhys. Lett. **5**, 413 (1988).

[4] R. Tao, J.T. Woestman, and N.K. Jaggi, Appl. Phys. Lett. **55**, 1844 (1989).

[5] J.E. Martin, J. Odinek, and T.C. Halsey, Phys. Rev. Lett. **69**, 1524 (1992).

[6] F. Richetti, J. Prost, and N.A. Clark, in *Electric Field Effects in Polyball Suspensions: Physics of Complex and Supermolecular Fluids*, edited by S.A. Safran and N.A. Clark (John Wiley & Sons, New York, 1987).

[7] L.D. Landau, E.M. Lifshitz, and L.P. Pitaevski, *Electrodynamics of Continuous Media*, 2nd ed. (Pergamon, New York, 1984), Chap. 5.

[8] T.C. Halsey and W. Toor, Phys. Rev. Lett. **65**, 2820 (1990); J. Stat. Phys. **61**, 1257 (1990).

[9] R. Tao and J.M. Sun, Phys. Rev. Lett. **67**, 398 (1991).

[10] T-j. Chen, R.N. Zitter, and R. Tao, Phys. Rev. Lett. **68**, 2555 (1992).

[11] Y.H. Hwang and X-l. Wu, Colloids Surf. A: Physiochem. Eng. Aspects **80**, 19 (1993).

[12] The particles were purchased from Seradyn, Inc., Indianapolis, IN 46206.

[13] M. Widom and H. Zhang, in *Complex Fluids*, edited by D. Weitz, E. Sirota, T. Witten, and J. Israelachvili, MRS Symposia Proceedings No. 248 (Materials Research Society, Pittsburgh, 1992), p. 235.

[14] The behavior is not due to a saturation in the magnetic susceptibility of the particles used. Such an effect will occur at a field at least one order of magnitude greater than our current experiment.

[15] To a good approximation the form and the structure factor can be mimicked by $P(q) \sim \exp(-\delta R^2 q^2)$ and $S(q) \sim 1/[q_0^4 + (q^2 - q_0^2)^2]$, respectively. Here $q_0 \sim 1/L_s$, with L_S being the mean distance between the domains. Maximizing $I(q) = P(q)S(q)$ with respect to q yields $q_{\max}/q_0 = F(\delta R^2/L_s^2)$, with $F(x) = \sqrt{1-x}$.

[16] While it is possible to observe the change in the column width as the particle concentration is varied, we found that it is difficult to measure the actual width of the columns because of smearing due to finite depth of view of the microscope.

[17] T.C. Halsey, Science **258**, 761 (1992).
[18] The magnetic field is quenched to a predetermined value over a time scale less than 1/100 seconds.
[19] G. Helgesen and A.T. Skjeltorp, *Spontaneous Formation of Space-Time Structure and Criticality* (Kluwer Academic Publisher, Dordrecht, 1991), p. 391; A.T. Skjeltorp, Phys. Rev. Lett. **51**, 2306 (1983).
[20] E. Lemaire, Y. Grasselli, and G. Bossis, J. Phys. (Paris) II **2**, 359 (1992).

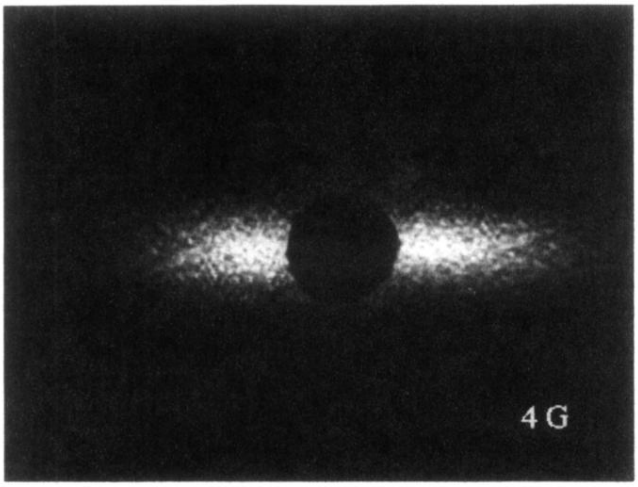

FIG. 2. Anisotropic scattering in the x-z plane. The concentration of the sample is $\phi = 5\%$ and the dimensionless sample thickness is $L/D = 25$. The optical anisotropy is a result of particle chaining along the z direction (vertical direction). The field (4 G) is applied adiabatically.

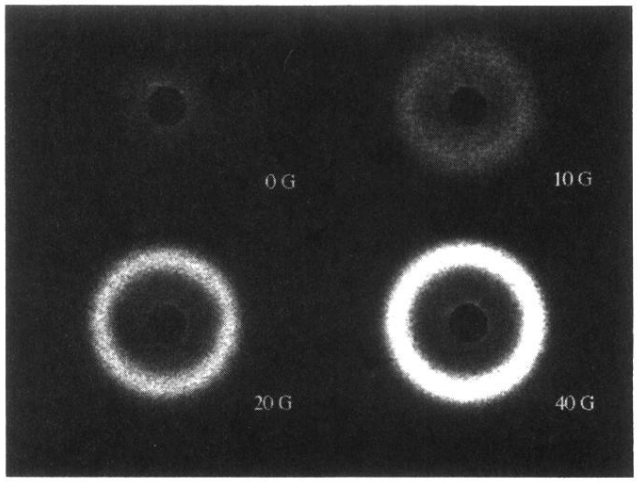

FIG. 4. The scattering intensity distribution in the x-y plane. The concentration of the sample is $\phi = 5\%$ and the sample thickness is $L/D = 25$. The magnetic field is applied adiabatically.